Available online at www.sciencedirect.com
SCIENCE DIRECT®
Journal of Molecular Catalysis A: Chemical 228 (2005) 283–291
JOURNAL OF MOLECULAR CATALYSIS A: CHEMICAL
www.elsevier.com/locate/molcata

Thermal decomposition of nickel acetate tetrahydrate: an integrated study by TGA, QMS and XPS techniques

Juan C. De Jesus[a,*], Ismael González[b], Angel Quevedo[b], Tito Puerta[b]

[a] *PDVSA-INTEVEP, Apdo. 76343, Caracas 1070A, Venezuela*
[b] *Escuela de Química, Facultad de Ciencias, Universidad Central de Venezuela, Apdo. 47102, Caracas 1040A, Venezuela*

Available online 24 November 2004

Abstract

The thermal decomposition of nickel carboxylates is a feasible route to synthesize metal nanoparticles suitable for catalytic purposes. The aim of this work is the characterization of the thermal decomposition course of nickel acetate tetrahydrate, $Ni(CH_3COO)_2{\cdot}4H_2O$. A thermogravimetric (TGA) decomposition study carried out in three different atmospheres (air, helium and hydrogen) showed that the dehydration of the parent salt occurs between 118 and 137 °C. However, irrespective of the chosen atmosphere, the sample weight loss registered in this stage remains invariable, suggesting the formation of a an intermediate basic acetate with the formula $0.86Ni(CH_3COO)_2{\cdot}0.14Ni(OH)_2$. The dehydration step was followed at ca. 350 °C by the subsequent one-step major decomposition of the acetate group, producing NiO and Ni, in treatment atmospheres of air and hydrogen, respectively, but there was some indication of an additional step when the thermolysis was conducted in helium. The conclusions possible from thermal analysis were confirmed by monitoring evolved gases employing quadrupole mass spectrometry (QMS), and a set of reactions linked to the decomposition of the acetate group has been proposed to account for most of the gas products detected. X-ray photoelectron spectroscopy (XPS) was used to investigate the solid phases obtained during the thermal decomposition of the salt in He atmosphere.

Keywords: Nickel acetate tetrahydrate; Decomposition; X-ray photoelectron spectroscopy; Thermogravimetric analysis; Quadrupole mass spectrometry

1. Introduction

The favoured method for preparation of supported catalysts is often referred as impregnation and drying, in which porous supports are impregnated with a solution of the active metal, followed by evaporation of the solvent and calcination in air to generate the oxidic phases that are precursors of the active (usually reduced) centers. Supported nickel catalysts comprise one of the most important class of heterogeneous catalysts, due to the widespread applications of these systems in a variety of applications, like methanation [1-3], partial oxidation [4,5], and steam reforming [6,7]. Nickel nitrate, which is widely used for the preparation of supported nickel catalysts, decomposes quantitatively to nickel oxide during the calcination step. There has been significant interest in studying the thermal decomposition of transition metal carboxylates, as potential sources of high surface area solids for catalysis, which demands particles in the range 1–3 nm for maximum efficiency and whose properties are strongly size dependent in this range. As a result, decomposition of pure nickel formate has been claimed recently to yield in a single step finely divided nickel metal with mean particle diameter of about 1.2 nm [8], and studies about the preparation and characterization of nickel-supported alumina employing aqueous solutions of nickel formate are now available [9]. Therefore, nickel carboxylates present an interesting alternative to conventional nitrate precursor, enabling the preparation of nickel-supported catalysts essentially through a one-step impregnation and decomposition mild route. In this sense, contributions to the knowledge of the surface structure of nickel nanoparticles obtained by thermal decomposition of carboxylate precursors are necessary to achieve the desired behavior on supported systems.

* Corresponding author.
E-mail address: dejesusjc@pdvsa.com (J.C. De Jesus).

1381-1169/$ – see front matter © 2004 Elsevier B.V. All rights reserved.
doi:10.1016/j.molcata.2004.09.065

Thermal decomposition of nickel acetate has been the subject matter of several previous studies [10–17]. Atmospheres employed so far include vacuum [10], flowing N_2 [11–17], dry oxygen [11], air [10,14], water [15], and self-generated atmospheres [16]. Solid residues covering intermediates and final products were characterized mainly by combining XRD and/or IR [10–15], and exceptionally employing NMR/SEM [16]. On the other hand, gases evolved concurrently during the thermal decomposition of nickel acetate have received limited consideration, they have been studied mainly by GC [11], IR [14], and MS [16,17]. In spite of the available information, there are still significant qualitative and quantitative differences reported for the mechanisms, solid intermediates and gases evolved during the thermal decomposition of nickel acetate [14].

In this paper we demonstrate the applicability of X-ray photoelectron spectroscopy (XPS), combined with studies of thermogravimetry (TGA) and temperature programmed decomposition studies with a quadrupole mass spectrometer (TPD-QMS), to the further characterization of the pyrolitic decomposition of nickel acetate tetrahydrate, $Ni(CH_3COO)_2{\cdot}4H_2O$.

2. Experimental

2.1. Materials

Commercially available nickel acetate tetrahydrate [$Ni(CH_3COO)_2{\cdot}4H_2O$] was used directly as the initial precursor for TGA, TPD and XPS studies.

2.2. Thermal analysis

TG measurements were carried out using a Cahn 2000 microbalance. Between 10 and 15 mg of sample were spread thinly over the quartz sample pan to minimize bed effects during decomposition of the nickel acetate samples. The heating rate was 30 °C/min, and the purge gas employed in all cases was He, at a flow of 45 ml/min. The treatment gas (He, Air and H_2) was admitted at 40 ml/min.

2.3. TPD analysis

TPD measurements were made in a purpose built quartz reactor of approximately 400 ml, connected through a leak valve and a heated capillary to an independently pumped Inficon Transpector quadrupole mass spectrometer operating under computer control. A nickel acetate tetrahydrate sample (10 mg), charged in the quartz reactor, was heated up to 1000 °C at 30 °C/min in He at a flow rate of 40 ml/min. The experiment was repeated several times to assure reproducibility of TPD data.

Preliminary analysis of the desorption process showed there are a significant amount of reaction products that contribute to a wide range of signals in the 0–100 AMU range, accessible with the quadrupole mass spectrometer employed. However, a careful analysis of published cracking patterns [18] justify the following suppositions, which to a great extent assist the identification of products and quantitative analysis of the desorption spectra [19]:

1. The signals at $m/e = 2$, 18, 25, 31, 37, 44, 56, 58, and 60 come up exclusively from the desorption of hydrogen, water, acetylene, ethanol, C_3H_4, CO_2, isobutylene, acetone, and acetic acid, respectively.
2. The signal at $m/e = 43$ receives contributions from both acetone and acetic acid, and is also characteristic of acetic anhydride, but after subtracting expected contributions it was determined that acetic anhydride production during thermal decomposition of NiAc in He is virtually zero.
3. The $m/e = 16$ peak is directly related to CH_4, after subtracting contributions from both water and CO_2.
4. After subtracting contributions from CH_4 and acetic acid, the $m/e = 14$ peak can be associated directly to ketene.
5. Formic acid can be related to $m/e = 46$, after subtracting ethanol contribution.
6. The $m/e = 28$, formally associated with CO, needs to be corrected by contributions arising from CO_2, formic acid and isobutylene.
7. The peak at $m/e = 30$ arises from both formaldehyde and ethane.

The application of accepted relative ionization gauge sensitivity factors, allowed the adjustment of intensity signals (Amps) acquired during the TPD runs, to obtain mol fractions as presented in Table 2.

2.4. XPS analysis

XPS spectra were recorded using a Leybold–Heraeus commercial surface analysis apparatus (LHS 11), equipped with a single channel detector, and employing AlKα radiation (1486.6 eV) at 360 W (power settings: 12 kV and 30 mA). The 100 mm radius hemispherical analyzer was set in the constant pass energy mode (pass energy = 200 eV). For XPS measurements, approximately 1 g of parent nickel acetate is placed in the quartz reactor, and heated linearly to the final temperature at 30 °C/min, in a dynamic atmosphere of He (40 ml/min). The sample is maintained over 60 min in the He atmosphere at the desired temperature, and cooled down to room temperature under flowing gas. The powdered samples are quickly removed, pressed, and mounted employing double sided tape. The normal operating pressure inside the turbo-pumped analysis chamber was kept below 5×10^{-8} Torr during data collection. Each spectral region was signal-averaged for a given number of scans to obtain good signal-to-noise ratios. Surface charging was observed on most samples, and accurate binding energies (BE) were determined by charge referencing by means of either adventitious carbon at 284.6 eV or with the reported value for metallic nickel component of 852.3 eV [20]; the BE were reproducible within ±0.2 eV. The photoelectron spectra were collected and stored in an interfaced

personal computer, using the SPECTRA 6.0 software from Specs GmbH.

2.5. Additional characterization

The total carbon content of the residue obtained after complete decomposition of 1 g of nickel acetate in the quartz reactor in a flow of He of 40 ml/min, heated from room temperature to 500 °C (30 °C/min) and maintained 15 min at the final temperature was measured by a C-400 (LECO Corp.) elemental analyser, having a carbon sensitivity of 0.01%.

3. Results

3.1. Thermogravimetric analysis

The results from the thermogravimetric measurements in flowing atmospheres of H_2, He and air are presented in the derivative form (DGA) in Fig. 1.The heating program in all cases was 25–700 °C at a rate of 30 °C/min. The values in percentage of weight retained (WR) at selected temperatures during the thermogravimetric analysis of the decomposition in a flow of He of nickel acetate tetrahydrate, are presented in Table 1. We can see that, under our experimental conditions, NiAc decomposition undergoes a maximum of three thermal processes, named as I–III in the weight derivative curves depicted in Fig. 1. Steps I and II are common to all treatments, but step III is only observable during inspection of the DGA curve obtained under He atmosphere (Fig. 1b).

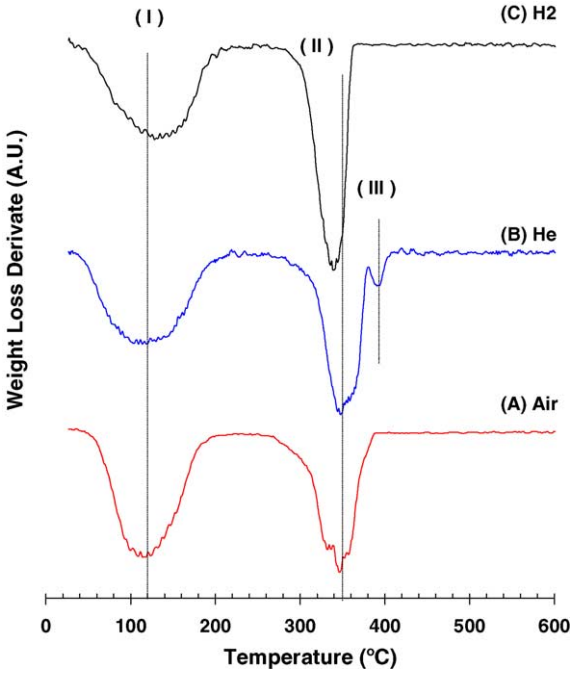

Fig. 1. Derivative thermogravimetric curves for the decomposition pf nickel acetate tetrahydrate, collected at 30 °C/min in He at 40 ml/min. Gas atmospheres employed are shown over each trace.

Table 1
Weight losses measured during TGA of NiAc (wt.%)

Temperature (°C)	H_2	Air	He
250	66.5	66.1	66.3
380	24.0	30.7	28.0
500	24.0	30.2	25.0

No matter of the treatment atmosphere employed during the thermal decomposition of NiAc, a broad peak with a T_{max} = 118–137 °C is registered in all the DGA curves; it can be assigned with a high degree of certainty to the dehydration of crystallized water in the initial precursor. After the dehydration is completed, the average for the WR at 250 °C recorded under the three different atmospheres (66.3%) is clearly below the value expected for the release of four water molecules (71.1%), indicating an evolution of additional amounts of material to the gas phase. Earlier reports suggest that hydrolysis of surface acetate groups is feasible during the dehydration of NiAc, resulting in simultaneous evolution of acetic acid to the gas phase, and generating basic nickel acetate in the solid phase, $(1-x)Ni(CH_3COO)_2{\cdot}xNi(OH)_2$) [11,13]. As will be shown below, our QMS results confirm the production of acetic acid during the dehydration step, as well as small amounts of additional by-products.

The step (II) in Fig. 1, with T_{max} = 345–350 °C, corresponds to the major decomposition of the dehydrated intermediate. Under H_2 atmosphere, the WR at 380 °C of 24.0% is consistent with the theoretical value for the formation of Ni (23.6%), while under air, the WR of 30.7% is compatible with the value expected for the formation of NiO (30.0%). At temperatures up to 500 °C, no additional changes in the weight of the residue are recorded in treatments of either H_2 or air atmospheres.

Interestingly, a third feature at T_{max} = 395 °C (step III, Fig. 1b) is clearly observed when the decomposition of NiAc is carried out in flowing He at atmospheric pressure. TGA experiments recorded at slightly higher pressures (data not shown) indicate that this process is pressure sensitive. The intermediate WR value of 28.0% measured at about 380 °C, suggests that a mixture of NiO and Ni is most likely obtained under an inert atmosphere. Further heating to 500 °C in He leads to a WR value of 25.0, slightly higher than the value calculated for the formation of pure Ni (23.6%). As will be discussed below, we believe this is due to carbonaceous species present on the surface of the metallic residue.

3.2. Gas evolved analysis

Information regarding the decomposition pattern of species generated during the pyrolisis of nickel acetate was obtained from temperature programmed decomposition (TPD) studies with a mass quadrupole (QMS). Mass spectra collected on-line during the decomposition of NiAc in He are shown in Figs. 2–5. Fig. 2 exhibits the curve obtained after adding the individual contributions for all the chemi-

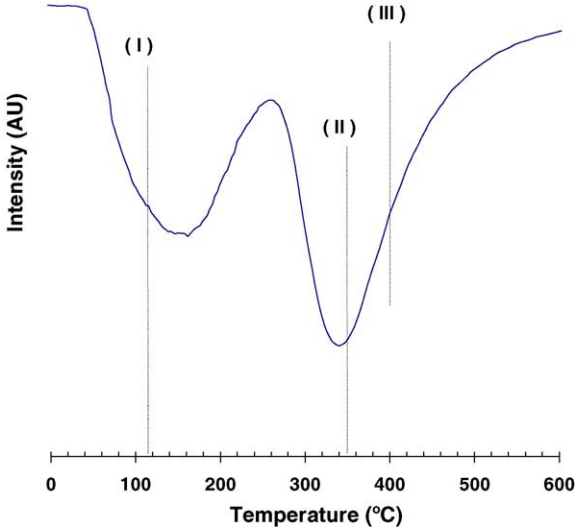

Fig. 2. Synthetic temperature-programmed decomposition trace, obtained after adding contributions for all gases identified by QMS during the thermal decomposition of nickel acetate tetrahydrate at 30 °C/min, in flowing He at 40 ml/min.

cal species identified by means of QMS. As a visual aid to help in the comparison with TGA data depicted in Fig. 1b, dotted lines are included in Fig. 2 at the same temperatures previously assigned for I–III decomposition steps. The curve resembles reasonably well the DGA displayed in Fig. 1b, corroborating most of the trends discussed previously for the thermal decomposition of NiAc under He atmosphere. The broad peak observed between ca. 50 and 240 °C in Fig. 2 can be related to the dehydration of NiAc, as explained before (step I, Fig. 1). As will be discussed below, it comprises different products besides water and acetic acid expected to form due to the surface hydrolysis of the acetate groups.

The major decomposition of NiAc, as indicated by a second broad peak extending from ca. 270 to 500 °C, is also

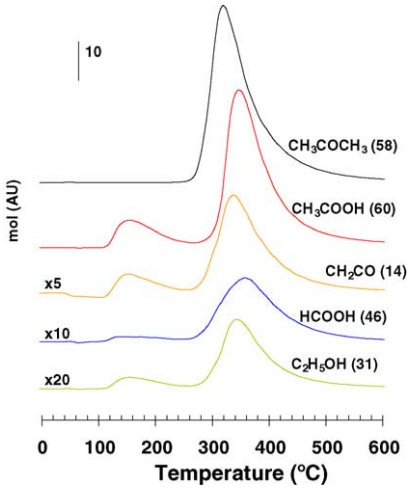

Fig. 3. Temperature-programmed decomposition spectra collected during linear heating of nickel acetate tetrahydrate, at a ramp of 30 °C/min in a flow of He at 40 ml/min (oxygenates, see text).

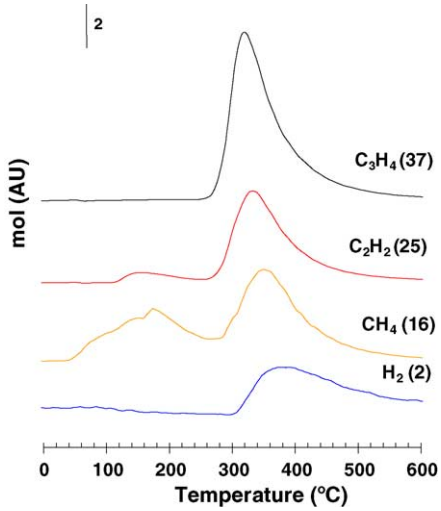

Fig. 4. Temperature-programmed decomposition spectra collected during linear heating of nickel acetate tetrahydrate, at a ramp of 30 °C/min in a flow of He at 40 ml/min (H_2 and hydrocarbons, see text).

evident in Fig. 2. However, the step III, clearly noticed previously during the TG analysis of the NiAc decomposition process in He, is not distinguished in the envelope of Fig. 2.

All the gases identified by QMS during the thermal decomposition of NiAc were conveniently detached in three main groups, namely oxygenates (Fig. 3), hydrogen + hydrocarbons (Fig. 4), and carbon oxides (Fig. 5). The water desorption trace is not reported because the corresponding signal at $m/e = 18$ is very broad, due to adsorption and possible some retention on the steel capillary. The relative product yields, based on the calibration of the TPD peak areas after correcting for coincident m/e values and conversion to partial pressures, are summarized in Table 2 and depicted in Fig. 6.

Ketene (CH_2CO), ethanol (CH_3CH_2OH), formic acid (HCOOH), acetic acid (CH_3COOH), and acetone (CH_3COCH_3), were unambiguously identified during the thermal decomposition of NiAc under He (see Fig. 3). As was settled before, hydrolisis of surface acetate groups most likely account for the observed production of acetic acid at

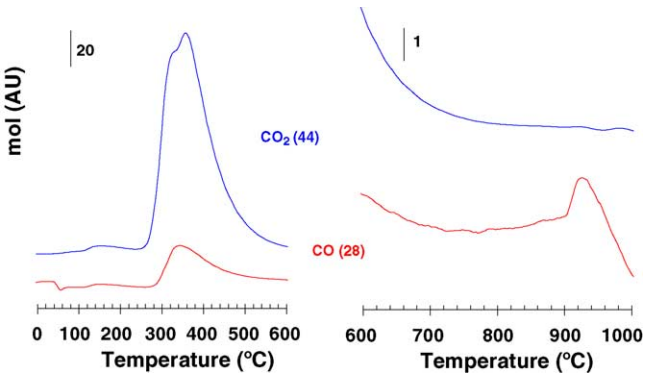

Fig. 5. Temperature-programmed decomposition spectra collected during linear heating of nickel acetate tetrahydrate, at a ramp of 30 °C/min in a flow of He at 40 ml/min (carbon oxides, see text).

Table 2
Product yields for nickel acetate decomposition in He

Desorption product	*m/e*	Yield fraction	Temperature (°C)
Hydrogen	2	0.113	394
Ketene	14	0.025	162
		0.195	344
Methane	16	0.119	182
		0.195	359
Water	18	7.440	162
		2.044	373
C_2H_2	25	0.019	162
		0.170	339
Carbon monoxide	28	1.000	350
		0.164	939
$HCHO + C_2H_6$	30	0.013	165
		0.044	350
Ethanol	31	0.006	162
		0.031	350
C_3H_4	37	0.277	327
Carbon dioxide	44	0.189	168
		6.289	339/365
Formic acid	46	0.006	162
		0.075	365
Isobutilene	56	0.003	197
		0.011	356
Acetone	58	1.541	327
Acetic acid	60	0.226	162
		1.390	353

ca. 150 °C. At this point, it is worth to mention that acetone production is not detected during the dehydration step.

Additionally, from the analysis of the spectra presented in Fig. 3, it is clear that during the major decomposition of the basic nickel acetate, acetone production is the first process at ca. 325 °C. At about 350 °C, an equivalent amount of acetic acid is desorbed, and there is also noticeable the releasing of minute amounts of ketene, formic acid, and ethanol.

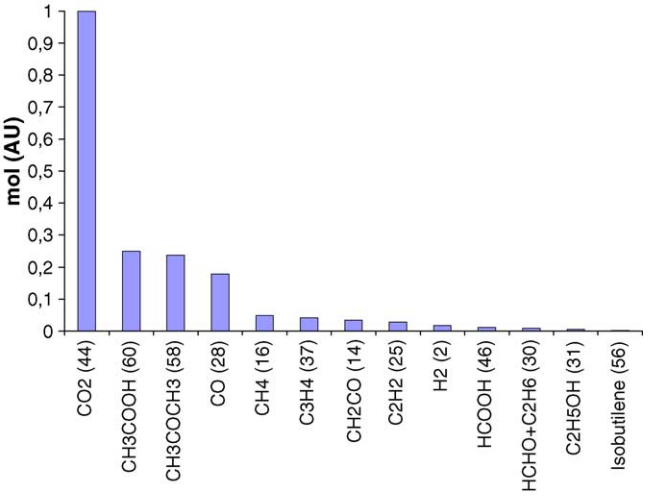

Fig. 6. Relative product yields for the thermal decomposition of nickel acetate tetrahydrate at 30 °C/min in a flow of He at 40 ml/min (see Table 2).

Mass spectra of hydrogen and hydrocarbons evolved during the decomposition of NiAc in He (Fig. 4), disclose that trace amounts of methane (CH_4) and ethylene (C_2H_4) are produced concurrently with oxygenated hydrocarbons at ca. 160 °C. During the major decomposition of the acetate group, a small amount of H_2 is also evolved to the gas phase at about 390 °C. Minute amounts of isobutilene were also detected during both the dehydration and the decomposition stages.

Carbon oxides are also produced during the thermal decomposition of nickel acetate tetrahydrated (see Fig. 5). While minute amounts of CO_x species are evolved during the dehydration step at ca. 150 °C, relatively high amounts of carbon oxides are produced between 280 and 500 °C, during the major decomposition step of the acetate group. Particularly, it is of interest to note that the the CO_2 trace in the left panel of Fig. 5 presents a distinguishing double structure, with peak maximum located at ca. 330 and 365 °C. Data showed in Table 2 and depicted in Fig. 6, clearly indicated that CO_2 is quantitatively the main product detected during the thermal decomposition of nickel acetate tetrahydrated. On the other hand, CO production is observed mainly at 350 °C, and interestingly is the only product detected as a trace at ca. 940 °C, as shown in the right panel of Fig. 5.

3.3. XPS analysis

The powders that result from the thermal decomposition of parent nickel acetate under He atmosphere were characterized employing X-ray photoelectron spectroscopy (XPS). Fig. 7 shows the relevant XPS spectra for pure nickel acetate

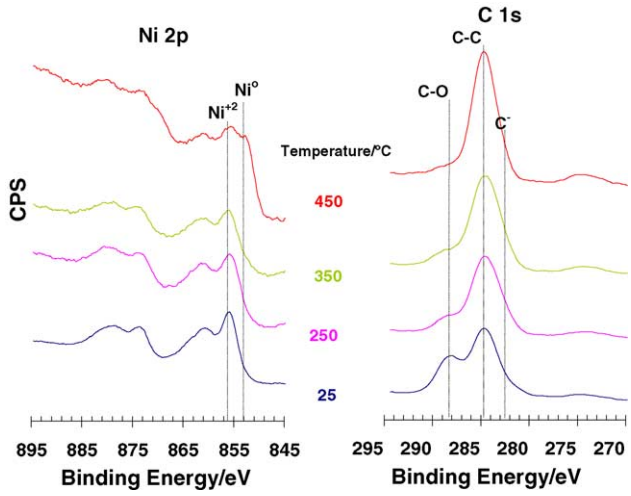

Fig. 7. X-ray photoelectron spectra collected during the thermal decomposition of nickel acetate tetrahydrate. The samples are heated in a quartz reactor in flowing He (40 ml/min) at a linear ramp of 30 °C/min, and maintained 60 min at the temperatures displayed over each trace, cooled at room temperature in the carrier gas, and transferred immediately to the instrument. Parent nickel acetate without any treatment is displayed as trace at 25 °C.

at 25 °C and residues collected at 300, 350 and 450 °C. The first observation to be addressed here is in fact that the C 1s XPS spectra displayed in the right panel of Fig. 7 display only two distinct peaks at binding energies around 288.2 and 284.6 eV. We can easily associate these two features with the carboxylate group and adventitious carbon, respectively. The carboxylate component diminishes strongly after heating to 300–350 °C, and virtually disappears on final heating to 450 °C. Notice, however, that the carbide component expected at around 283.3 eV [21] is not apparent upon examination of the C 1s XPS spectra displayed on Fig. 7, ruling out the formation of surface nickel carbides, as reported previously by others accordingly to XRD analysis of the residues [11].

The changes perceivable on the corresponding Ni 2p spectra are, however, much more subtle. The overall shape of the Ni 2p XPS line proved to be virtually unaffected upon heating of the nickel acetate to temperatures up to 350 °C, as showed in the left panel of Fig. 7. However, TGA and TPD data suggest that very important chemical changes must be accounted for in this temperature range. On the other hand, intense color changes are observable upon treatment, from bright green for the parent nickel acetate tetrahydrated, to green-yellowish to the basic nickel acetate (300 °C) and black for both residues collected at 350 and 450 °C. In these series of experiments, the Ni 2p spectra are characterized mostly by a main peak at around 855.5 eV, as well as very intense satellites at the higher binding energy side of the main peaks, both characteristic of Ni^{2+} ion. A large amount of Ni^{2+} species are reported around the obtained value of 855.5 eV, including nickel acetate, $NiCO_3$, $Ni(OH)_2$, and NiO [22]. Therefore, assuming that the overall XPS signal of nickel in the 25–350 °C temperature range may originate from multiple Ni^{2+} species, the identification of the nickel states is not as straightforward as in the case of the C 1s XPS.

The best approach is just to focus on the changes observable in the Ni 2p region for the sample treated at 450 °C (Fig. 7, top). There, a new component at around 852.5 eV clearly develops, in agreement with the formation of metallic nickel as proposed before from the analysis of TGA and TPD data.

4. Discussion

4.1. Thermogravimetry

Our quantitative TGA results confirm previous findings indicating that the decomposition of nickel acetate tetrahydrated is critically controlled by the reaction atmosphere [14]. As shown in Table 1, by comparing the results obtained for the thermal decomposition of the parent salt in H_2 with those obtained in air, it is possible to propose the formation of either metallic nickel or NiO, respectively. Nonetheless, from a mechanistic point of view, the characterization of the decomposition process under an inert atmosphere of He is much more challenging, because an additional step suggests the involvement of a NiO/Ni mixture as a likely intermediate.

Therefore, we focus our attention to the events associated with the thermal decomposition process of the nickel acetate precursor under an inert He atmosphere. Table 1 reveals that the average mass value retained after step I under different atmospheres (66.3%) is well below that expected for stoichiometric loss of four water molecules (71.1%). Our values are lower than the ones reported elsewhere in a static atmosphere of air (69.3%) [14], and under dynamic atmospheres of N_2, (68%) in [11] and (72%) in [12]. On the other hand, Galwey et al. [16] measured a mass loss almost identical to the one reported in our work, after heating in vacuum a commercial sample of nickel acetate for 2 h at 470 K; they interpreted the result as if the precursor salt were pentahydrated instead of tetrahydrated.

Our understanding of the thermogravimetric results allows a supplementary reading of the extra weight loss obtained during the dehydration step. Dorémieux [17] first suggested the possible formation of a basic acetate as intermediate compound $[(1-x)NiAc_2{\cdot}xNi(OH)_2]$ in his pioneering work, and in considering the value of WR obtained systematically in our work for the residue of step (I), we can assume the stoichiometry of the hydrolisis reaction to allow roughly an estimation of the x value for the formation of basic nickel acetate, permitting the following chemical reaction to be proposed:

$$Ni(CH_3COO)_2 \cdot 4H_2O = 0.86Ni(CH_3COO)_2 \cdot 0.14Ni(OH_2) + 0.28CH_3COOH + 3.72H_2O \quad (1)$$

Therefore, the production of 0.28 mol of acetic acid would explain the difference in weight loss observed experimentally here, and may also account very well for the evolution of an additional water molecule, as interpreted alternatively by Galwey et al. [16].

4.2. Gas evolved analysis

One of the key observations reported in this paper is the fact that our TPD-QMS studies corroborate on-line the simultaneous production of both water and acetic acid during the dehydration step of nickel acetate tetrahydrated. In addition, other oxygenated hydrocarbons, as ketene, formic acid, and ethanol, were also detected at ca. 120 °C, as shown in Fig. 3. The similar temperature and peak shape for all these four products suggest that they were derived from the same surface species through equivalent reaction channels, accordingly with the following trend (see Table 2 and Fig. 6):

$$CH_3COOH > CH_2CO > CH_3CH_2OH \gg HCOOH$$

Alternatively, the oxygenates produced during the dehydration step may be due to the following set of reactions, presumably involving gas phase homogeneous transforma-

tions of the acetic acid:

$$CH_3COOH = CH_2CO + H_2O \quad (2)$$

$$CH_3COOH + H_2 = CH_3CH_2OH \quad (3)$$

$$2CH_3COOH = 2HCOOH + C_2H_4 \quad (4)$$

Whichever mechanism is responsible for the production of ketene, ethanol and formic acid during the dehydration step, it is clear that only a fraction of all the acetic acid formed by hydrolysis is detected. The water to acetic acid ratio measured during the dehydration step (see Table 2) is well above the one expected through the fulfillment of reaction (2) (33 versus 13). This figures imply that approximately 60% of all the acetic acid generated initially by surface acetate hydrolysis is transformed to by-products through decomposition reactions like (2)–(4).

It should nevertheless be pointed out here that it is well known that undesirable side reactions between gases may also take place at some extent at the ionizer of mass quadrupoles, and quantification with this instruments is not always straightforward; for instance, the purpose of the gas analysis presented in this study is to speculate on possible mechanisms and achieve a reasonable comparison with experimental data available in the literature.

One more important observation, evident from the analysis of the acetone trace depicted in Fig. 3, needs to be highlighted here. The fact that acetone production during the dehydration step is virtually zero, rules out the occurrence at low temperatures of the following ketonysation reaction, reported elsewhere during the acid catalyzed decomposition of acetic acid, and feasible at temperatures close to the one reported here for the dehydration step [23]:

$$2CH_3COOH = CH_3COH_3 + CO_2 + H_2O \quad (5)$$

In addition to oxygenates, minute amounts of methane and CO_2 are also observed concurrently during the dehydration step, although in much lower concentrations, as shown in Fig. 4 and left panel of Fig. 5, respectively. In fact, methane and CO_2 production at ca. 160–190 °C can be explained through the following reaction:

$$CH_3COOH = CH_4 + CO_2 \quad (6)$$

Following the same approach as before, next we will address the issue of the major decomposition process, observed in this work around 340 °C by TGA (Fig. 1) and corroborated by means of TPD-QMS studies (Fig. 2), in very good agreement with data reported elsewhere [11,14].

As seen in Fig. 3, acetone is the first oxygenated produced at ca. 325 °C during the major decomposition of the acetate group. Then, at about 350 °C, acetic acid is detected, as well as minute amounts of ketene, formic acid and ethanol, virtually the same products observed previously during the dehydration step. CO_2 is clearly the main product observed during the thermal decomposition of nickel acetate (see Table 2). The acetone production, as well as the double structure observed for the CO_2 trace depicted in the left panel of Fig. 5, can be conveniently explained with the following set of reactions:

$$Ni(CH_3COO_2 = NiCO_3 + CH_3COCH_3\,(330\,^\circ C) \quad (7)$$

$$NiCO_3 = NiO + CO_2\,(330\,^\circ C) \quad (8)$$

$$NiO + CO = Ni + CO_2\,(373\,^\circ C) \quad (9)$$

The peak temperatures reported here for the production of CO_2 are in good agreement with previous results obtained during the thermal decomposition of nickel acetate in air [14]. Acetone generation, on the other hand, supports the formation in the solid phase of $NiCO_3$, as suggested in a previous work [14]. We believe $NiCO_3$ is a short-lived intermediate that decarboxylates immediately to give NiO, as proposed in 8.

On the other hand, it is difficult to understand by what mechanism the acetate group decomposes to yield gaseous acetic acid as a product [12]. However, it has been pointed out that the major gaseous product of the decomposition of acetates of reducible metal ions (e.g. nickel acetate) is acetic acid [24].

Autocatalytic NiO reduction to metallic nickel is the key observation reported in the literature in the case of nickel carboxylate decomposition [16]. In the present work, CO reduction of NiO is proposed through reaction (9), but, the formation of H_2, observed in Fig. 4 at temperatures above 300 °C with a peak maximum around 390 °C, may also contribute to the quantitative reduction of intermediate NiO, through the following reaction:

$$NiO + H_2 = Ni + H_2O \quad (10)$$

We also believe that this reaction is responsible for the step III (see Fig. 1b), noticed during themogravimetric analysis of the decomposition of nickel acetate tetrahydrated in He, because a broad water signal is produced at high temperatures with a peak temperature of around 373 °C (see Table 2).

On the other hand, the water detected at higher temperatures could be also in part the result of the dehydration of the basic portion of the proposed intermediate:

$$Ni(OH)_2 = NiO + H_2O\,(370–390\,^\circ C) \quad (11)$$

The TPD results summarized in Table 2 and depicted in Fig. 6, suggest that carbon oxides and oxygenates are the main products of the thermal decomposition of nickel acetate tetrahydrated, with the following trend:

$$CO_2 > CH_3COCH_3 > CH_3COOH > CO > CH_2CO$$

This is in contrast with the results of Mohamed [11] who reported a very different trend, carrying out the decomposition in a similar manner under an inert N_2 atmosphere, but employing gas chromatography for the characterization of the gases evolved:

$$CH_3COOH > CO_2 \gg CH_3COCH_3$$

We believe that this divergence is more likely related to differences in the technique employed for gas-evolved analysis (i.e. gas chromatography versus mass quarupole).

4.3. X-ray photoelectron spectroscopy

The discussion provided so far suggests some possible intermediates and products for the thermal decomposition of nickel acetate, based solely on the interpretation of weight losses and the complementary analysis of evolved gases by means of TPD-QMS. Further insight into the chemical composition of the solids generated at different stages can be obtained taking advantage of the power of XPS as a surface sensitive technique, as compared to XRD, habitually employed for solid characterization.

Besides the parent nickel acetate, our TGA and TPD-QMS findings suggest the involvement of at least $Ni(OH)_2$, $NiCO_3$, NiO, and Ni, during the course of the thermal decomposition of nickel acetate. Furthermore, there is some uncertainty as to whether nickel carbide is as well a reaction intermediate and/or retained in the final decomposition product during the pyrolisis of NiAc [11,16].

The XPS data reported in the results section reveal that surface carbides are not detected as steady species along the thermal decomposition treatment, in contrast with previous XRD results. It is well known that the surface sensitivity of XPS allows the detection of chemical states otherwise imperceptible by bulk analysis techniques as XRD, and this may account for the differences observed in the present work. We nevertheless favor the results suggested here, because it has been pointed out that nickel carbide is metastable and quickly decomposed on heating close or above 400 °C [25].

TGA and TPD-QMS analysis indicated an almost complete reduction of nickel acetate to metallic nickel, when the thermolysis was carried out at 450 °C in He atmosphere. On the other hand, XPS complementary analysis, as shown in the left side panel of Fig. 7 (top), still indicate important contributions of Ni^{2+} species on the surface of the metallic residue.

Our samples were not specially preserved, and in this condition natural passivation of elemental metals is expected even after brief exposures to the atmosphere [26]. On the other hand, metallic nickel nanoparticles are expected to be very reactive, and the build-up of a relatively thick nickel oxide/hydroxyde film is feasible immediately upon air exposure [27].

XPS analysis confirm that highly reactive metallic nickel is obtained directly as the final product of the thermal decomposition of nickel acetate, under an inert He atmosphere and at temperatures higher than 400 °C. Independent carbon analysis showed that the product contained 4–5% of carbon, while TPD data depicted in Fig. 5 (right side panel) suggests that the carbonaceous species present on the surface of the nickel particles react at 940 °C, evolving minute amounts of CO to the gas phase.

We are at present investigating the catalytic activity of the nickel particles obtained after the thermal decomposition of nickel acetate tetrahydrate, and also exploring alternative ways of characterizing their physicochemical properties.

5. Conclusions

On linear heating, nickel acetate tetrahydrate first releases water at ca. 120 °C, but acetic acid is produced concurrently due to the surface hydrolysis of the constituent anion. During the dehydration step, gas phase reactions of the acetic acid produce mainly ketene, and minute amounts of ethanol and formic acid. Basic nickel acetate, with an estimated formula $0.86Ni(CH_3COO)_2{\cdot}0.14Ni(OH)_2$, is proposed as an intermediate following the dehydration step, as suggested by interpretation of thermogravimetric data. On continued heating, the subsequent decomposition of the basic nickel acetate at ca. 340 °C lead directly to the formation of either NiO or Ni, under treatment atmospheres of air and H_2, respectively. In an inert atmosphere, however, an additional step suggests that NiO is intermediate to the final production of metallic Ni with an estimated 4–5% of carbonaceous residues. While the evolution of acetone during the major decomposition step suggests the involvement of $NiCO_3$ as a short-lived intermediate, acetic acid production may be an indication of the final reduction to metallic nickel. In contrast to previous reports, carbides were not detected in the surface as intermediates during the thermal decomposition of nickel acetate by XPS analysis.

Acknowledgements

Finantial support for this research was provided by PDVSA-Intevep.

References

[1] M. Agnelli, H.M. Swaan, C. Marquez-Alvarez, G.A. Martin, C. Mirodatos, J. Catal. 175 (1998) 117.
[2] A.E. Aksoylu, Z. Onsan, Appl. Catal. A Gen. 164 (1997) 1.
[3] I. Alstrup, J. Catal. 151 (1995) 216.
[4] R. Jin, Y. Chen, W. Li., W. Cui, Y. Ji, C. Yu, Y. Jiang, Appl. Catal. A Gen. 201 (2000) 71.
[5] Z. Liu, K. Jun, H. Roh, S. Baek, S. Park, J. Mol. Catal. A: Chem. 189 (2002) 283.
[6] H.S. Bengaard, J.K. Norskov, J. Sehested, B.S. Clauser, L.P. Nielsen, A.M. Molenbroek, J.R. Rostrup-Nielsen, J. Catal. 209 (2002) 365.
[7] T. Borowiecki, A. Golebiowski, B. Stasinska, Appl. Catal. A. Gen. 153 (1997) 141.
[8] A.B. Edwards, C.D. Garner, K.J. Roberts, J. Phys. Chem. B 101 (1997) 20.
[9] A.N. Kharat, P. Pendleton, A. Badalyan, M. Abedini, M.M. Amini, J. Catal. 205 (2002) 7.
[10] P. Baraldi, Spectrosc. Acta A 38 (1982) 51.
[11] M.A. Mohamed, S.A. Halawy, M.M. Ebrahim, J. Anal. Appl. Pyrolysis 27 (1993) 109.
[12] M. Afzal, P.K. Butt, H. Ahmad, J. Therm. Anal. 37 (1991) 1015.
[13] A.M. Gadalla, H.F. Yu, Thermochim. Acta 164 (1990) 21.
[14] G.A.M. Hussein, A.K.H. Nohman, K.M.A. Attyia, J. Therm. Anal. 42 (1994) 1155.
[15] N. Nishizawa, T. Kishikawa, H. Minami, J. Sol. State Chem. 146 (1999) 39.
[16] A.K. Galwey, S.G. McKee, T.R.B. Mitchell, React. Sol. 6 (1988) 173.

[17] J.L. Doremieux, Bull. Soc. Chim. Fr. 5 (1969) 1508.
[18] The Mass Spectrometry Data Centre (Eds.), Eight Peak Index of Mass Spectra, The Royal Society of Chemistry, Nottingham, 1983.
[19] M.L.M. Bonati, R.W. Joyner, M. Stockenhuber, Catal. Today 81 (2003) 653.
[20] C.D. Wagner, W.M. Riggs, L.E. Davis, J.F. Moulder, G.E. Muilenberg (Eds.), Handbook of X-Ray Photoelectron Spectroscopy, Perkin–Elmer, Eden Prairie, 1978.
[21] N. Laidani, L. Calliari, G. Speranza, V. Michelli, E. Galvanetto, Surf. Coat. Tech. 100–101 (1998) 116.
[22] L.J. Matienzo, L.I. Yin, S.O. Grim, W.E. Swartz, Inorg. Chem. 12 (12) (1973).
[23] O. Kresnawahjuesa, R.J. Gorte, D. White, J. Mol. Catal. A 208 (2004) 175.
[24] N.E. Fouad, M.A. Mohamed, M.I. Zaki, H. Knozinger, J. Anal. Appl. Pyrolysis 53 (2000) 185.
[25] J.P. Coad, J.C. Riviere, Surf. Sci. 3 (1961) 609.
[26] T.L. Barr, J. Phys. Chem. 16 (1982) 1801.
[27] X. Phung, J. Groza, E.A. Stach, L.N. Williams, S.B. Ritchey, Mater. Eng. A 359 (2003) 261.